Editors' Suggestion Featured in Physics

Route to a Superconducting Phase above Room Temperature in Electron-Doped Hydride Compounds under High Pressure

Ying Sun,[1] Jian Lv,[1] Yu Xie,[1] Hanyu Liu,[1,*] and Yanming Ma[1,2,†]

[1]*Innovation Center of Computational Physics Methods and Software and State Key Laboratory for Superhard Materials, College of Physics, Jilin University, Changchun 130012, China*

[2]*International Center of Future Science, Jilin University, Changchun 130012, China*

(Received 24 December 2018; published 26 August 2019)

The recent theory-orientated discovery of record high-temperature superconductivity ($T_c \sim 250$ K) in sodalitelike clathrate LaH_{10} is an important advance toward room-temperature superconductors. Here, we identify an alternative clathrate structure in ternary Li_2MgH_{16} with a remarkably high estimated T_c of ~473 K at 250 GPa, which may allow us to obtain room-temperature or even higher-temperature superconductivity. The ternary compound mimics a Li- or electron-doped binary hydride of MgH_{16}. The parent hydride contains H_2 molecules and is not a good superconductor. The extra electrons introduced break up the H_2 molecules, increasing the amount of atomic hydrogen compared with the parent hydride, which is necessary for stabilizing the clathrate structure or other high-T_c structures. Our results provide a viable strategy for tuning the superconductivity of hydrogen-rich hydrides by donating electrons to hydrides via metal doping. Our approach may pave the way for finding high-T_c superconductors in a variety of ternary or quaternary hydrides.

DOI: 10.1103/PhysRevLett.123.097001

Superconductivity in a known hydride was first reported in 1970, when Th_4H_{15} was identified to have a T_c of 8 K at ambient pressure [1]. An important direction towards which to search for high-temperature superconductors in hydrogen-rich metal hydrides was proposed by considering that hydrogen in a high content can play a critical role in the creation of the superconductivity of the compounds [1]. However, this approach was not widely adopted until Ashcroft's suggestion [2] that high-pressure conditions can metallize hydrogen-rich materials that are insulators at ambient pressure. Subsequently, there has been much research on hydrogen-rich hydrides under high pressures [3–6]. Breakthroughs were achieved in SH_3 and LaH_{10} systems, which had high T_c of ~200 and 250–260 K, respectively [7–13].

Theoretical studies have been crucial in these discoveries. Solid SH_2 was predicted to transform into a high-temperature superconductor above 100 GPa [7]. Subsequent experimental work found two superconducting states with T_c of 30–150 and ~200 K, where isotope effect measurements indicated that the materials were Bardeen-Cooper-Schrieffer superconductors [8]. The superconductivity at ~200 K was explained by SH_3 arising from the decomposition of SH_2 under high pressure [9,14–18]. SH_3 adopts a cubic structure with two interpenetrating perovskite sublattices, where atomic H is located symmetrically between each pair of S atoms and forms strong sixfold polar covalent S-H bonds. This three-dimensional network of covalently bonded H appears only in SH_3 [8,9] and SeH_3 [19,20].

Two theoretical studies have predicted high superconductivity in sodalitelike clathrate LaH_{10} at $T_c \sim 280$ K above a pressure of 2 Mbar [10,11]. Two subsequent experiments synthesized the predicted stoichiometry and $Fm\bar{3}m$ structure of LaH_{10} and measured high superconductivities of $T_c = 260$ and 250 K at high pressures of 190 and 170 GPa, respectively [12,13], setting a record high T_c for superconductors. In clathrate LaH_{10}, the bonds between H and La atoms are purely ionic, whereas the H atoms form sodalitelike clathrate cages consisting of weakly covalent H-H bonds with a H-H distance of ~1.2 Å. A similar H clathrate structure was first proposed for CaH_6 [21] and was found to be ubiquitous in alkaline-earth and rare earth hydrides [10,11,22,23]. The high superconductivity of these clathrate hydrides arises from H atoms, where the H electrons contribute substantially to the electron density of states at the Fermi level [10,11,21–23]. Thus, clathrate hydrides are the most promising candidates for room-temperature superconductors.

Nearly all binary hydrides have been investigated by structure searching simulations [3–5], among which, the ionic clathrate structure in rare-earth and alkali-earth hydrides [10,11,21–23] and the covalent sixfold cubic structure in SH_3 [8,9] and SeH_3 [19] give the highest possible T_c values above 200 K. There are many other binary hydrides, some of which have even higher H content, (e.g., MgH_{12} [24], MgH_{16} [24], YH_{24} [10], and AsH_8 [25]); however, the predicted T_c values are much lower ($T_c < 150$ K). These hydrides contain a large amount of H_2-like or H_3-like (e.g., KH_5 [26]) molecular

units, in which the H electrons occupy the low-lying bonding orbits (σ) that are far from the Fermi level. Consequently, the electron densities of states at the Fermi level are low in these hydrides, even though the H content is higher. High-T_c superconductivity relies on intramolecular H-H bonds being broken to have H electrons in energy states near the Fermi level. To achieve this, extra electrons can be introduced via metal doping into the system, allowing the antibonding states of H_2 or H_3 molecules to accept electrons for dissociation of the molecules [4,6,10,21].

There have been few studies on the superconductivity of compressed ternary hydrides [27–40]. Experimental examples include $BeReH_9$ [27] and Li_5MoH_{11} [28] synthesized under high-pressure conditions and showing unexpectedly low $T_c < 10$ K. Crystal structure prediction simulations for ternary systems are computationally demanding. Theoretically studied ternary systems can be mainly classified as variants of the cubic SH_3 structure [29–33] and substitutional alloys of MH_6 ($M = \mathrm{Ca,\ Y}$) [34,35], and their T_c values are generally lower than those of LaH_{10} (~280 K) and YH_{10} (~303 K) [10,11]. Searching for room-temperature or higher-temperature superconductors among the ternary hydrides remains a challenging but pressing task.

This Letter proposes a strategy for designing high-temperature superconductors through introducing extra electrons via metal doping into known hydrogen-rich binary systems that contain abundant H_2 or H_3 molecular-like units. The role of the extra electrons is to break up the H molecules to make atomic hydrogen more abundant than the parent phase, which is necessary for stabilizing high-T_c structures [6,10,21]. We use lithium-doped magnesium hydrides as the model system, because the parent MgH_{16} system contains a large amount of H_2 molecules [24] and Li has a similar atomic radius to Mg but a smaller electronegativity, allowing a larger charge transfer from Li to H.

The high-pressure ternary phase diagram of the Li-Mg-H system is constructed through extensive structure searching simulations via the swarm intelligence-based CALYPSO method [41,42]. There is a nearly linear correlation between the number of electrons accepted per H_2 unit and H-H separation, implying a trend on the creation of atomic H via metal doping in binary hydrides. The results also reveal a unique clathrate structure with a stoichiometry of Li_2MgH_{16} and an unprecedented highest T_c of 473 K at 250 GPa.

We examine the phase diagram of $Li_xMg_yH_z$ at 300 GPa [Figs. 1(a) and S1 [43]], focusing on H-rich species. Although all ternary hydrides are thermodynamically stable against dissociation into pure elements [61–63], they are metastable phases with respect to decomposition into the energetically most favorable binary phases [24,64]; for example, for Li_2MgH_{16}, the lowest enthalpy is

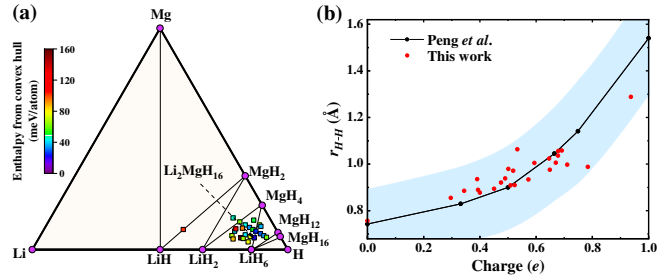

FIG. 1. (a) Calculated stabilities of three-component $Li_xMg_yH_z$ relative to Li [61], Mg [62], and H [63] at 300 GPa. Colored squares denote metastable phases (above the convex hull, see Supplemental Material [43], Fig. S1). Purple circles indicate stable phases [24,64]. Black lines between purple circles connect stable phases. (b) Variation of the H-H separation ($r_{\mathrm{H\text{-}H}}$) in a H_2 molecule with the electrons accepted per H_2 molecule in the Li-Mg-H system at 300 GPa.

~20 meV/atom above the convex hull (Fig. S1 [43]). This metastability does not preclude these materials from experimental synthesis. According to the inorganic crystal structure database, 20% of experimentally synthesized materials are metastable, some of which even have high positive formation enthalpies with high energy gains larger than 40 meV/atom [65,66]. For Li_2MgH_{16}, we also propose a synthetic route through the chemical reaction of LiH, MgH_2, and H_2, where the calculated formation enthalpy is highly negative, at −84 meV/atom at 300 GPa.

We examine the electronic properties of $Li_xMg_yH_z$ based on crystal structure. Bader charge analysis reveals a large charge transfer from Li/Mg to H [52], suggesting that both Li and Mg are electron donors and bonding is ionic between H and Li/Mg atoms. To investigate the H-H bonding character, we calculate the integrated crystalline orbital Hamiltonian population (ICOHP) [50] for H-H pairs to characterize the orbital interaction between two H atoms. For various ICOHP values, where stronger H-H bonds (shorter $r_{\mathrm{H\text{-}H}}$) give larger negative values (Fig. S2 [43]), Fig. 1(b) shows a nearly linear correlation between the average Bader charges per H_2 and the average $r_{\mathrm{H-H}}$ of the strongest H-H bonds in the Li-Mg-H system at 300 GPa, which is consistent with previous reports [10]. If the number of electrons accepted per H_2 reaches $0.6e$, the H_2 molecule readily dissociates as the H-H bond length increases to about 1.0 Å, which is similar to the H-H distance (0.98 Å) in monatomic solid hydrogen at 500 GPa [67]. This result is also supported by a direct comparison of the child structure of Li_xMgH_{16} ($x = 1$, 2, and 3) with its parent structure of MgH_{16} at 300 GPa (Table S1 [43]), where the H-H distance increases with increasing Li content.

The stoichiometry of Li_2MgH_{16} (with a space group of $P\bar{3}m1$) has the lowest enthalpy, but is ~20 meV/atom above the convex hull of the $Li_xMg_yH_n$ compounds (Fig. S1 [43]). The calculated enthalpies as a function of

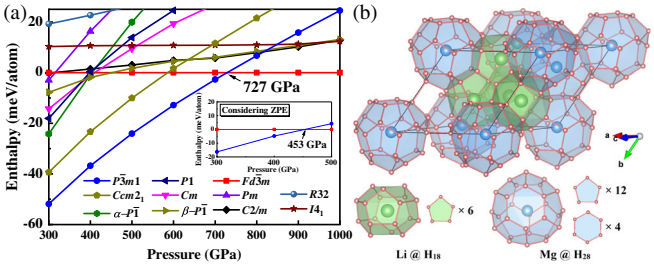

FIG. 2. (a) Calculated enthalpy as a function of pressure for predicted structures relative to the $Fd\bar{3}m$ phase. Inset: Calculated enthalpy with considering zero-point energy (ZPE) as a function of pressure. (b) Clathrate structure of Li_2MgH_{16} with the space group $Fd\bar{3}m$ at 300 GPa, consisting of Li-centered H_{18} cages and Mg-centered H_{28} cages. Each H_{18} or H_{28} cage consists of 6 or 12 pentagons and 4 hexagons.

pressure are shown in Fig. 2(a). The most stable phase in the pressure range of 300–727 GPa is $P\bar{3}m1$, consisting of partially dissociated H_2 units (0.83 and 0.98 Å, at 300 GPa) [Fig. S3(a) [43]]. Above 727 GPa, an unusual clathrate structure [space group $Fd\bar{3}m$, Fig. 2(b)], which contains Li-centered H_{18} cages and Mg-centered H_{28} cages and no H_2 units, becomes the ground state. Each H_{18} or H_{28} cage consists of 6 or 12 pentagons and 4 hexagons, with H-H bond lengths of 1.02, 1.08, and 1.20 Å, respectively, although the electron localization result indicates that the H-H bonds are covalent (Fig. S4 [43]). Because of the high vibrational frequency arising from light elements, the zero-point motion is critical in determining the phase stabilities. Compared with the atomic H in the $Fd\bar{3}m$ phase, the H_2 molecular units in the $P\bar{3}m1$ phase produce higher-frequency phonons. Thus, there is a large energy difference (30 meV/atom) between $P\bar{3}m1$ and $Fd\bar{3}m$ structures, which is similar to that between molecular [63] and atomic hydrogen [67] at 500 GPa (29 meV/atom, Table S2 [43]). Consequently, the phase transition between $P\bar{3}m1$ and $Fd\bar{3}m$ occurs at a substantially lower pressure of 453 GPa at 0 K [Fig. 2(a), inset]. The absence of an imaginary frequency in the phonon spectra indicates that the clathrate structure is dynamically stable above 250 GPa (Fig. S10 [43]). Moreover, the high temperature can help to stabilize the $Fd\bar{3}m$ structure further if compared with $P\bar{3}m1$ (Fig. S11 [43]), indicating that the $Fd\bar{3}m$ phase may be realized at high temperature.

All the predicted Li-Mg-H ternaries are metallic at 300 GPa, as confirmed by the electronic band structure calculations. In particular, $Fd\bar{3}m$-Li_2MgH_{16} (Fig. S12 [43]) has the highest H-dominated electronic density of states at the Fermi level (N_{Ef}) that is almost twice that of MgH_{16} (Fig. S13 [43]) at 300 GPa. Therefore, we investigate its superconductive properties further. The calculated electron-phonon coupling parameter (λ) of Li_2MgH_{16} is as high as 3.35 [Fig. 3(c)]. This value is much higher than those of MgH_{16} and any other Li-Mg-H ternary compound

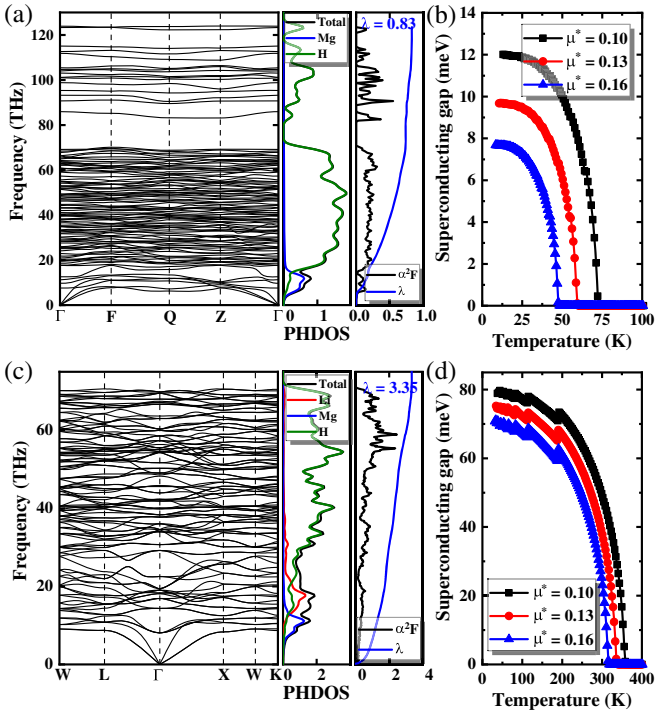

FIG. 3. Phonon dispersion relations, projected phonon densities of states (PHDOS), and Eliashberg spectral function for (a) Li_2MgH_{16} ($P\bar{1}$) and (c) Li_2MgH_{16} ($Fd\bar{3}m$) at 300 GPa. Calculated anisotropic superconducting gap of (b) MgH_{16} ($P\bar{1}$) and (d) Li_2MgH_{16} ($Fd\bar{3}m$) at 300 GPa.

(Table S1 [43]). The bending modes of atomic H (20–72 THz) contribute 50% of the total λ, and Mg (below 15 THz) and Li atoms (10–20 THz) contribute 40% and 10%, respectively. There is no high-frequency vibration, consistent with the absence of molecular H_2 units in the structure. The highest phonon frequency (72 THz, 2400 cm^{-1}) can also be compared with other systems containing atomic H, such as 2600 cm^{-1} in the $I4_1/amd$ phase of metallic hydrogen at 500 GPa [67], and 2300 cm^{-1} in the $Fm\bar{3}m$-LaH_{10} phase at 300 GPa [10,11]. The Eliashberg equation [60] gives a better description of systems with strong electron-phonon coupling for $\lambda > 1.5$. The T_c values are evaluated through the direct numerical solution of the Eliashberg equation. Clathrate-structured Li_2MgH_{16} is predicted to be a potential room-temperature superconductor with an estimated T_c value of up to 351 K with a typical Coulomb pseudopotential parameter $\mu^* = 0.1$ at 300 GPa [Fig. 3(d)]. Under the same conditions, the calculated T_c value is much smaller at 73 K for MgH_{16} [Fig. 3(b)] due to the existence of the high content of H_2 units. In particular, $Fd\bar{3}m$-Li_2MgH_{16} is dynamically stable down to 250 GPa (Fig. S10 [43]). N_{Ef} decreases upon decompression, whereas λ increases (Fig. 4). The T_c value of $Fd\bar{3}m$-Li_2MgH_{16} at 250 GPa is predicted to be even higher at around 430–473 K, with μ^* in the range of 0.16 to 0.1 (Fig. S14 [43]).

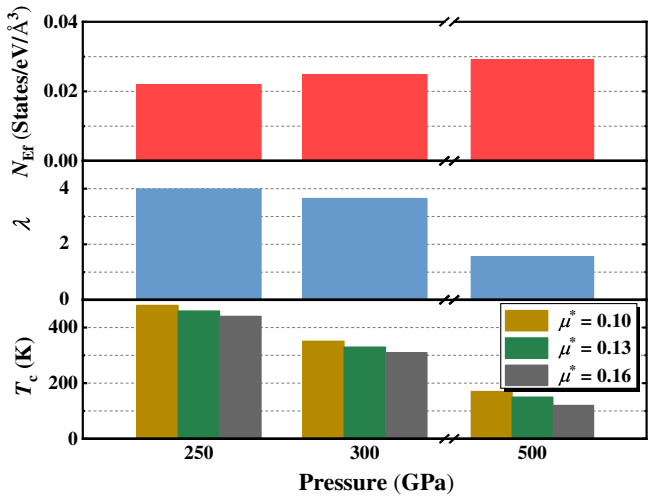

FIG. 4. Calculated electronic density of states at the Fermi level (N_{Ef}) per cubic Angstrom (top panel), the electron-phonon coupling parameter (λ) (middle panel), and T_c (bottom panel) of Li_2MgH_{16} ($Fd\bar{3}m$) at 250, 300, and 500 GPa, respectively.

As part of efforts to develop electron-doped superhydrides, we design a potential room-temperature ternary superconductor of $Fd\bar{3}m$-Li_2MgH_{16}, although the predicted synthetic pressure (~250 GPa) is high. We note that this is the first ternary example of using our method, and we expect that investigations of other ternary systems may identify other high-temperature superconductors at pressures much lower than the current one. It is known that anharmonicity is important in the calculation of the T_c in many compressed hydrides [14,68]. However, simulations with anharmonic effects are not performed since they are computationally demanding and will not fundamentally revise the high superconductivity of the $Fd\bar{3}m$ structure.

In summary, we propose a method for designing new ternary high-temperature superconductors via introducing metal elements into parent hydrides that contain a large amount of H_2 molecules. The doping dissociates H_2 molecules into atomic H, substantially increasing the electron density of states at the Fermi level, and consequently increasing T_c. Lithium-doped magnesium hydrides were studied as model systems to support our method. We found a nearly linear correlation between electrons accepted per H_2 and H-H distance, and the clathrate structure of Li_2MgH_{16} is predicted to be a potential room-temperature superconductor with an estimated T_c of up to 473 K at 250 GPa. Our current results provide a useful route for designing room-temperature superconductors under high pressure, and we expect that the method will stimulate further experimental and theoretical studies for exploration of a large variety of hydrogen-rich ternary or quaternary hydrides.

This work is supported by the National Natural Science Foundation of China (Grant No. 11534003), Science Challenge Project No. TZ2016001, the Fundamental Research Funds for the Central Universities (Jilin University, JLU), the Program for JLU Science and Technology Innovative Research Team (JLUSTIRT), and National Key Research and Development Program of China (under Grant No. 2016YFB0201201). We used the computing facilities at the High-Performance Computing Centre of Jilin University and Tianhe2-JK at the Beijing Computational Science Research Centre.

Y. S., J. L., and Y. X. contributed equally to this work.

*hanyuliu@jlu.edu.cn
†mym@jlu.edu.cn

[1] C. B. Satterthwaite and I. L. Toepke, Phys. Rev. Lett. **25**, 741 (1970).
[2] N. W. Ashcroft, Phys. Rev. Lett. **92**, 187002 (2004).
[3] T. Bi, N. Zarifi, T. Terpstra, and E. Zurek, in *Reference Module in Chemistry, Molecular Sciences and Chemical Engineering* (Elsevier, New York, 2019).
[4] H. Wang, X. Li, G. Y. Gao, Y. W. Li, and Y. M. Ma, WIREs Comput. Mol. Sci. **8**, e1330 (2018).
[5] J. A. Flores-Livas, L. Boeri, A. Sanna, G. Profeta, R. Arita, and M. Eremets, arXiv:1905.06693.
[6] L. Zhang, Y. Wang, J. Lv, and Y. Ma, Nat. Rev. Mater. **2**, 17005 (2017).
[7] Y. Li, J. Hao, H. Liu, Y. Li, and Y. Ma, J. Chem. Phys. **140**, 174712 (2014).
[8] A. P. Drozdov, M. I. Eremets, I. A. Troyan, V. Ksenofontov, and S. I. Shylin, Nature (London) **525**, 73 (2015).
[9] D. Duan, Y. Liu, F. Tian, D. Li, X. Huang, Z. Zhao, H. Yu, B. Liu, W. Tian, and T. Cui, Sci. Rep. **4**, 6968 (2014).
[10] F. Peng, Y. Sun, C. J. Pickard, R. J. Needs, Q. Wu, and Y. Ma, Phys. Rev. Lett. **119**, 107001 (2017).
[11] H. Liu, I. I. Naumov, R. Hoffmann, N. W. Ashcroft, and R. J. Hemley, Proc. Natl. Acad. Sci. U.S.A. **114**, 6990 (2017).
[12] M. Somayazulu, M. Ahart, A. K. Mishra, Z. M. Geballe, M. Baldini, Y. Meng, V. V. Struzhkin, and R. J. Hemley, Phys. Rev. Lett. **122**, 027001 (2019).
[13] A. P. Drozdov *et al.*, Nature (London) **569**, 528 (2019).
[14] I. Errea, M. Calandra, C. J. Pickard, J. Nelson, R. J. Needs, Y. Li, H. Liu, Y. Zhang, Y. Ma, and F. Mauri, Phys. Rev. Lett. **114**, 157004 (2015).
[15] Y. Li *et al.*, Phys. Rev. B **93**, 020103(R) (2016).
[16] N. Bernstein, C. S. Hellberg, M. D. Johannes, I. I. Mazin, and M. J. Mehl, Phys. Rev. B **91**, 060511(R) (2015).
[17] D. F. Duan, X. L. Huang, F. B. Tian, D. Li, H. Y. Yu, Y. X. Liu, Y. B. Ma, B. B. Liu, and T. Cui, Phys. Rev. B **91**, 180502(R) (2015).
[18] M. Einaga, M. Sakata, T. Ishikawa, K. Shimizu, M. I. Eremets, A. P. Drozdov, I. A. Troyan, N. Hirao, and Y. Ohishi, Nat. Phys. **12**, 835 (20016).
[19] S. Zhang, Y. Wang, J. Zhang, H. Liu, X. Zhong, H. F. Song, G. Yang, L. Zhang, and Y. Ma, Sci. Rep. **5**, 15433 (2015).
[20] J. A. Flores-Livas, A. Sanna, and E. K. U. Gross, Eur. Phys. J. B **89**, 63 (2016).

[21] H. Wang, J. S. Tse, K. Tanaka, T. Iitaka, and Y. Ma, Proc. Natl. Acad. Sci. U.S.A. **109**, 6463 (2012).
[22] Y. Li, J. Hao, H. Liu, J. S. Tse, Y. Wang, and Y. Ma, Sci. Rep. **5**, 9948 (2015).
[23] X. L. Feng, J. R. Zhang, G. Y. Gao, H. Y. Liu, and H. Wang, RSC Adv. **5**, 59292 (2015).
[24] D. C. Lonie, J. Hooper, B. Altintas, and E. Zurek, Phys. Rev. B **87**, 054107 (2013).
[25] Y. H. Fu, X. Du, L. Zhang, F. Peng, M. Zhang, C. J. Pickard, R. J. Needs, D. J. Singh, W. Zheng, and Y. Ma, Chem. Mater. **28**, 1746 (2016).
[26] J. Hooper and E. Zurek, J. Phys. Chem. C **116**, 13322 (2012).
[27] T. Muramatsu, W. K. Wanene, M. Somayazulu, E. Vinitsky, D. Chandra, T. A. Strobel, V. V. Struzhkin, and R. J. Hemley, J. Phys. Chem. C **119**, 18007 (2015).
[28] D. Z. Meng, M. Sakata, K. Shimizu, Y. Iijima, H. Saitoh, T. Sato, S. Takagi, and S. I. Orimo, Phys. Rev. B **99**, 024508 (2019).
[29] Y. F. Ge, F. Zhang, and Y. G. Yao, Phys. Rev. B **93**, 224513 (2016).
[30] C. Kokail, W. von der Linden, and L. Boeri, Phys. Rev. Mater. **1**, 074803 (2017).
[31] D. Li, Y. Liu, F. B. Tian, S. L. Wei, Z. Liu, D. F. Duan, B. B. Liu, and T. Cui, Front. Phys. **13**, 137107 (2018).
[32] B. B. Liu *et al.*, Phys. Rev. B **98**, 174101 (2018).
[33] M. Amsler, Phys. Rev. B **99**, 060102(R) (2019).
[34] X. Liang, A. Bergara, L. Wang, B. Wen, Z. Zhao, X. F. Zhou, J. He, G. Gao, and Y. Tian, Phys. Rev. B **99**, 100505(R) (2019).
[35] H. Xie, D. Duan, Z. Shao, H. Song, Y. Wang, X. Xiao, D. Li, F. Tian, B. Liu, and T. Cui, J. Phys. Condens. Matter **31**, 245404 (2019).
[36] S. Zhang, L. Zhu, H. Liu, and G. Yang, Inorg. Chem. **55**, 11434 (2016).
[37] J. A. Flores-Livas, A. Sanna, M. Grauzinyte, A. Davydov, S. Goedecker, and M. A. L. Marques, Sci. Rep. **7**, 6825 (2017).
[38] Y. Ma, D. Duan, Z. Shao, D. Li, L. Wang, H. Yu, F. Tian, H. Xie, B. Liu, and T. Cui, Phys. Chem. Chem. Phys. **19**, 27406 (2017).
[39] Y. B. Ma, D. Duan, Z. Shao, H. Yu, H. Liu, F. Tian, X. Huang, D. Li, B. Liu, and T. Cui, Phys. Rev. B **96**, 144518 (2017).
[40] M. Rahm, R. Hoffmann, and N. W. Ashcroft, J. Am. Chem. Soc. **139**, 8740 (2017).
[41] Y. C. Wang, J. A. Lv, L. Zhu, and Y. M. Ma, Phys. Rev. B **82**, 094116 (2010).
[42] Y. C. Wang, J. Lv, L. Zhu, and Y. M. Ma, Comput. Phys. Commun. **183**, 2063 (2012).
[43] See Supplemental Material at http://link.aps.org/supplemental/10.1103/PhysRevLett.123.097001 for computational details, phase diagrams, electronic structures, phonon dispersion curves, mean squared displacement, and structural parameters of all predicted Li-Mg-H compounds,which includes Refs. [38,39,44–60].
[44] G. Kresse and J. Furthmuller, Phys. Rev. B **54**, 11169 (1996).
[45] P. E. Blochl, Phys. Rev. B **50**, 17953 (1994).
[46] J. P. Perdew, K. Burke, and M. Ernzerhof, Phys. Rev. Lett. **77**, 3865 (1996).
[47] J. P. Perdew and Y. Wang, Phys. Rev. B **46**, 12947 (1992).
[48] P. Blaha, K. Schwarz, P. Sorantin, and S. B. Trickey, Comput. Phys. Commun. **59**, 399 (1990).
[49] F. Birch, Phys. Rev. **71**, 809 (1947).
[50] R. Dronskowski and P. E. Bloechl, J. Phys. Chem. **97**, 8617 (1993).
[51] V. L. Deringer, A. L. Tchougreeff, and R. Dronskowski, J. Phys. Chem. A **115**, 5461 (2011).
[52] R. F. W. Bader, Acc. Chem. Res. **18**, 9 (1985).
[53] A. D. Becke and K. E. Edgecombe, J. Chem. Phys. **92**, 5397 (1990).
[54] K. Parlinski, Z. Q. Li, and Y. Kawazoe, Phys. Rev. Lett. **78**, 4063 (1997).
[55] A. Togo, F. Oba, and I. Tanaka, Phys. Rev. B **78**, 134106 (2008).
[56] P. Giannozzi *et al.*, J. Phys. Condens. Matter **21**, 395502 (2009).
[57] S. Baroni, S. de Gironcoli, A. Dal Corso, and P. Giannozzi, Rev. Mod. Phys. **73**, 515 (2001).
[58] D. R. Hamann, M. Schluter, and C. Chiang, Phys. Rev. Lett. **43**, 1494 (1979).
[59] F. Giustino, M. L. Cohen, and S. G. Louie, Phys. Rev. B **76**, 165108 (2007).
[60] G. M. Eliashberg, ZhETF **38**, 966 (1960) [Sov. Phys. JETP **11**, 696 (1960)].
[61] J. Lv, Y. Wang, L. Zhu, and Y. Ma, Phys. Rev. Lett. **106**, 015503 (2011).
[62] H. Olijnyk and W. B. Holzapfel, Phys. Rev. B **31**, 4682 (1985).
[63] C. J. Pickard and R. J. Needs, Nat. Phys. **3**, 473 (2007).
[64] E. Zurek, R. Hoffmann, N. W. Ashcroft, A. R. Oganov, and A. O. Lyakhov, Proc. Natl. Acad. Sci. U.S.A. **106**, 17640 (2009).
[65] Y. B. Wu, P. Lazic, G. Hautier, K. Persson, and G. Ceder, Energy Environ. Sci. **6**, 157 (2013).
[66] Y. Hinuma *et al.*, Nat. Commun. **7**, 11962 (2016).
[67] J. M. McMahon and D. M. Ceperley, Phys. Rev. Lett. **106**, 165302 (2011).
[68] W. Sano, T. Koretsune, T. Tadano, R. Akashi, and R. Arita, Phys. Rev. B **93**, 094525 (2016).